IEEE Transactions on Nuclear Science, Vol. NS-26, No. 3, June 1979

COMPUTER MODELING OF THE GYROCON*

Paul J. Tallerico and James E. Rankin
Los Alamos Scientific Laboratory, Los Alamos, NM 87545

Abstract

We discuss a gyrocon computer model in which the electron beam is followed from the gun output to the collector region. The initial beam may be selected either as a uniform circular beam or may be taken from the output of an electron gun simulated by the program of William Herrmannsfeldt. The fully relativistic equations of motion are then integrated numerically to follow the beam successively through a drift tunnel, a cylindrical rf beam deflection cavity, a combination drift space and magnetic bender region, and an output rf cavity. The parameters for each region are variable input data from a control file. The program calculates power losses in the cavity wall, power required by beam loading, power transferred from the beam to the output cavity fields, and electronic and overall efficiency. Space-charge effects are approximated if selected. Graphical displays of beam motions are produced. We discuss the Los Scientific Laboratory (LASL) prototype design as an example of code usage. The design shows a gyrocon of about two-thirds megawatt output at 450 MHz with up to 86% overall efficiency.

Introduction

The gyrocon is a deflection-modulated rf amplifier (Fig. 1) for the vhf to microwave range with potentially very high efficiencies at very high powers for cw or pulsed operation. A solid electron beam from a klystron-like electron gun is deflected by a rotating rf field. The beam forms a solid helix but individual electron motion is almost purely radial and vertical, i.e., not rotary. The deflection is increased by a static magnetic field (the bender) until the beam is moving roughly perpendicular to the original axis. The beam crosses the slotted, annular output cavity approximately normal to the flow of a traveling rf wave around the cavity. The beam crossing zone keeps pace with the wave. The beam electrons transfer their energy to the rf fields and parameters may be adjusted to virtually stop the electrons. Thus, high dc-to-rf conversion efficiencies are possible.

This basic concept, without the bender, was patented by McRae,[1] in 1946, as a frequency multiplier. Kaufman and Ottman,[2] in 1965, built a frequency multiplier that generated 0.4 W of power at 34 GHz with a 65-W drive power at 8.5 GHz. Their device had a linear output cavity, a length of shorted rectangular guide. Their paper contains several references to unpublished work on similar devices in the 1950's. In 1958, P. B. Wilson,[3] at Stanford University, theoretically investigated a large family of deflection-modulated devices, including the gyrocon, but no devices were built.

More recently G. I. Budker,[4,5] at the Institute for Nuclear Research in Novisibirsk, studied these concepts and constructed a 430-MHz pulsed gyrocon and a 181-MHz cw gyrocon. In this cw model, the 1-MW beam was made relativistic at 250 kV, the bender solenoid was added to increase the beam deflection, magnetic beam focusing was included at the output cavity through additional coils, and the beam was injected into the output cavity at a predetermined deviation from normal incidence to increase energy extraction. This deviation is produced and controlled by the bender and focusing fields that introduce some electron angular motion about the central gyrocon axis. Measured overall efficiencies up to 75% are claimed.

Mathematical Model

Solution Method and Assumptions

The gyrocon computer code numerically integrates the relativistic equations of motion with the external electromagnetic fields given by analytic expressions for the deflection and output cavities. Static fields caused by current loops in the solenoid or the focus coils are also included in all regions. Self fields caused by beam space charge are also approximately included in all regions. The electron gun is handled separately by an electron gun program.[6]

No aperture or fringing field effects are included in the field expressions for the gyrocon code. Image-charge effects are ignored in calculating space-charge fields. Only one charge disk of electrons is actually followed by the simulation. The beam is assumed to be homogeneous so that neighboring disks behave in essentially similar fashion except for differences in time, angle, etc. This method allows a full beam to be approximately constructed from the behavior of one disk. Finally, the self fields used in space-charge calculations are derived using Coulomb's Law and Ampere's Law for the self fields of

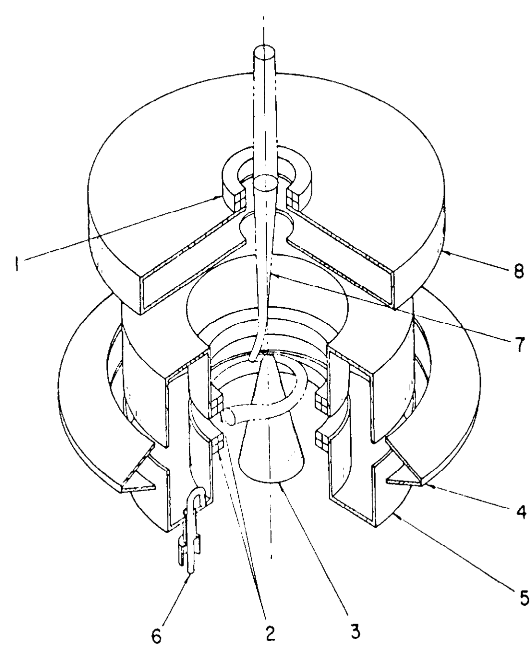

Fig. 1. The radial gyrocon:
(1) gun focus coil,
(2) output focal coils,
(3) bender,
(4) collector,
(5) output cavity,
(6) RF output,
(7) electron beam, and
(8) deflection cavity.

*Work supported by the U. S. Department of Energy.

0018-9499/79/0600-4015$00.75 © 1979 IEEE

charge elements. Thus, these fields are approximated to first order in v/c.

RF Deflection Cavity

The basic deflection modulation of the gyrocon beam occurs in a cylindrical rf cavity located below the electron gun (Fig. 1). The deflection cavity is driven at the fundamental device frequency. The computer code can simulate the incoming beam either by constructing a homogeneous ideal beam of given size, current, and voltage or by accepting the beam predicted by Herrmannsfeldt's electron optics program. The deflection is accomplished by driving the cavity in the TM_{110} mode at two points 90^{o} out of phase, thus producing a rotating rf field. In the cavity center, the mode appears approximately as a constant magnitude, transverse magnetic field rotating at the drive frequency. This field causes the desired rotating deflection by bending the beam around the magnetic field lines. The drive power required is that consumed by the cavity walls plus beam loading power, the latter calculated from the change in the beam energy as it traverses the cavity. Beam loading occurs because the electric field in the TM_{110} mode is not exactly zero over the entire beam.

Bender Effects

To reduce the drive power required for beam deflection and to obtain a horizontal beam at the output cavity, Budker included the solenoidal magnetic beam bender (Fig. 1). Its fields are produced by horizontal current loops[7] centered around the gyrocon axis. These fields cause the electrons to bend at increasing angles toward the output cavity. The bender fields and the focus coil fields introduce some electron motion about the gyrocon axis. This motion causes the beam to enter the output cavity at some deviation from a purely radial direction. The angle of deviation is advantageously used in Budker's design, as noted earlier.

The code uses the expression for the current loop fields to simulate these fields and includes their presence in all regions the beam traverses.

Focus Coils

To retard beam expansion in the output cavity, Budker included current loops on either side of the output cavity slot. These loops are parallel to the slot and encircle the gyrocon axis (Fig. 1). Reverse currents excite these loops so that the field between them in the slot and across the output cavity resembles a solenoid field along the beam motion, at least in the z direction. Although the field is axially symmetric, it does provide beam focusing in the vertical direction. The code simulates this field in the same manner as it treats the bender fields.

Additional focus coils in the gun or collector regions are generally included to provide better beam control.

Output Cavity

The output cavity field is simulated as a traveling rf wave in the TE_{111} mode. This technique considers the cavity to be a shorted coaxial waveguide with the wave circulating around the central axis.[8] The beam radially traverses the cavity. Both the beam and the traveling wave rotate at the same velocity. The cavity's electric field opposes the electron motion and thus extracts energy as it slows the electrons. The code calculates the rf output power, which is the power lost by the beam minus the power lost in the cavity walls. Output phase is adjustable and must be set for maximum beam energy extraction. After leaving the cavity, the beam drifts until all disk positions have emerged. An extended drift region may simulate a collector.

Space-Charge Fields

To calculate space-charge effects the beam helix is simulated by a bundle of charged rods lying along the actual helix. Each rod moves approximately with the average velocity of the charge disk. The helical beam motion reduces the linear charge density and decreases the space charge. The motion also compresses the rods into a more compact bundle and this compression increases the space-charge fields. Using Coulomb's Law, each rod is assigned an electric field and a magnetic field. The fields from all the rods are superposed to yield the approximate space-charge fields. The charge densities vary inversely with the disk component velocities because the charge density increases as the beam slows down. This increase is offset partially by the increased helical beam motion. This entire method keeps the space-charge calculations relatively simple.

LASL Prototype Gyrocon

The LASL prototype gyrocon has a 450-MHz frequency. The electron optics program[6] predicts a 9-A electron beam at 86 kV with good qualities for transport through the 450-MHz deflection cavity. The beam then passes through the bender drift space, between the focus coils, through the 450-MHz output cavity, and into the collector (Figs. 2 and 3). The magnetic fields from the bender and focus coils can be seen in the contours of Fig. 2. The deflection cavity is 8-cm long with a 40.6-cm radius. The output cavity extends radially from 16 cm to 23 cm and has an end-to-end height of 39.8 cm. The slot in the output cavity is 8.7-cm wide. A second set of focus coils positioned astride the collector region provides beam control in the collector. For optimum performance the polarities of the two sets of focus coils are reversed.

Beam and Disk Dynamics

Side and top views of disk motion (Figs. 2 and 3) display the distortions experienced by the disk passing through the system. These figures show individual

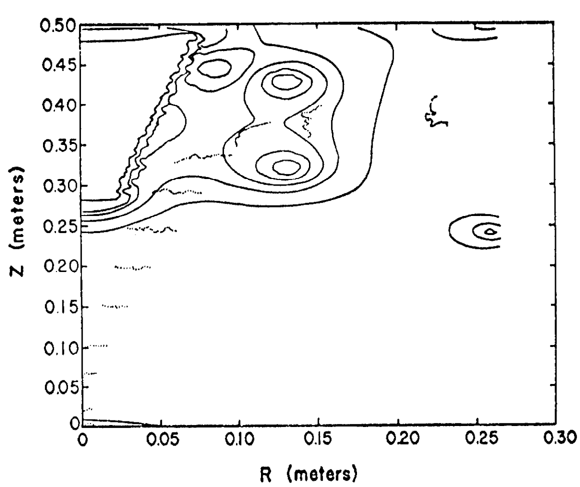

Fig. 2. Magnetic contours and disk motion in the LASL prototype gyrocon.

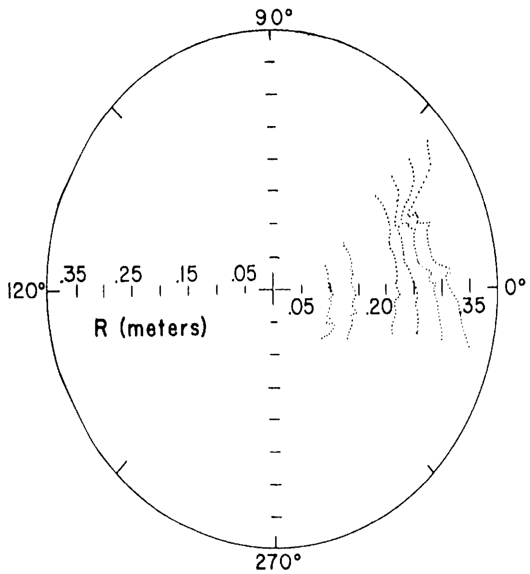

Fig. 3. Top view of disk motion in the LASL prototype.

disks at selected times during the run. The top view shows the beam occupies no more than about 60° in the output cavity and has far better bunching than klystrons. The angle at which the disk enters the output cavity is also visible. This angle of deviation from the normal is caused by the bender and focus fields. Because the output cavity fields push the beam back toward the normal, this deviation is desirable.

General Performance Trends

Table I summarizes current computer predictions of 450-MHz gyrocon performance over a wide range of operating conditions. Note that the higher beam powers produce higher overall efficiencies. The gyrocon is optimally a high-power device. For a given beam power, there is a beam voltage that gives a maximum efficiency, while for higher voltages the cavity wall losses decrease the efficiency. There is an optimum perveance of approximately 0.1 micropervs, and for a given perveance, most computer runs indicate that overall efficiency increases monotonically with beam voltage. The overall efficiency and rf gain cannot be maximized simultaneously.

Conclusions

A gyrocon computer model using simplified space-charge calculations describes gyrocon operation. The calculations indicate that high-power, high-efficiency gyrocons can operate in the 450-MHz region, and that efficiency increases with beam power. Computations for the LASL prototype indicate an 86% dc-to-rf conversion efficiency for a 9-A, 86-kV electron beam.

TABLE I

450-MHz GYROCON PERFORMANCE SUMMARY WITH A 1-cm INITIAL BEAM RADIUS

V_o (kV)	I_o (A)	a (cm)	b-a (cm)	Electronic Efficiency	P_ℓ (kW)	Overall Efficiency	P_{out} (kW)	rf Gain
100-kW Beam Power								
50	2.0	14	7	0.8872	10.6	0.7187	78.1	8.9
100	1.0	14	7	0.9026	28.3	0.5852	61.9	10.6
200	0.5	14	12	0.4803	23.1	0.2389	24.9	5.9
500	0.2	14	18	0.0989	4.5	0.0506	5.4	0.9
1000	0.1	14	18	0.0312	1.7	0.0126	1.5	0.1
300-kW Beam Power								
50	6.0	17	7	0.8582	11.6	0.7522	245.9	8.9
100	3.0	14	7	0.9615	33.5	0.8149	254.9	19.8
200	1.5	9	8	0.9626	62.8	0.7332	226.0	27.5
500	0.6	10	18	0.7384	96.4	0.3993	125.1	9.4
1000	0.3	9	24	0.1945	19.5	0.1277	38.8	9.4
1000-kW Beam Power								
100	10.0	14	7	0.9135	45.5	0.8329	868.0	20.6
200	5.0	10	10	0.9559	61.5	0.8848	894.4	83.0
500	2.0	10	16	0.9381	188.8	0.7378	749.3	48.3
1000	1.0	14	19	0.3017	149.2	0.1490	152.6	6.5
3000-kW Beam Power								
100	30.0	14	7	0.8514	45.5	0.8058	2508.7	22.2
200	15.0	16	11	0.9269	77.3	0.8830	2703.3	43.8
500	6.0	14	15	0.9096	228.8	0.8283	2499.9	137.1
1000	3.0	14	18	0.7459	968.3	0.4197	1269.4	51.6
10000-kW Beam Power								
200	50.0	13	7	0.8231	167.2	0.7548	8064.8	11.8
500	20.0	18	14	0.9426	359.5	0.8975	9067.3	88.9
1000	10.0	13	18	0.9549	793.3	0.8700	8756.1	136.5
2000	5.0	13	19	0.8647	2464.9	0.6112	6181.6	53.9

Acknowledgments

We thank Barbara E. Canada for diligently calculating the results shown in Table I. We also thank Dr. J. V. Lebacqz of Stanford Linear Accelerator Center for many helpful suggestions.

References

1. J. W. McRae, "Harmonic Generation System," U. S. Patent No. 2 408 436, October 1946.
2. I. Kaufman and G. Oltman, "Harmonic Generation by Electron Beam Pattern Motion - the Bermutron," IEEE Trans. on Electron Devices, ED-12, pp. 31-39, January 1965.
3. P. B. Wilson, "Notes on Trajectory-Modulated Electron Devices," Microwave Laboratory report 527, W. W. Hansen Laboratory of Physics, Stanford University, June 1956.
4. G. I. Budker et al., "Microwave Electron Discharge Device," U. S. Patent No. 3 885 193, May 1975, and U. S. Patent No. 4 019 088, April 1977.
5. G. I. Budker et al., "The Gyrocon - A High Efficiency Powerful Energy Converter with a Relativistic Electron Beam for High Frequency Acceleration of Charged Particles," Atomic Energy, Vol. 44, pp. 397-403, May 1978.
6. W. B. Herrmannsfeldt, "Electron Trajectory Program," Stanford Accelerator Linear Accelerator publication SLAC-166 (1973).
7. R. F. Harrington, Introduction to Electromagnetic Engineering (McGraw Hill, New York, 1958).
8. S. Ramo and J. R. Whinnery, Fields and Waves in Modern Radio, second edition (John Wiley and Sons, New York, 1964), pp. 364-366.